

Lennard-Jones systems near solid walls: Computing interfacial free energies from molecular simulation methods

Ronald Benjamin and Jürgen Horbach

*Institut für Theoretische Physik II, Heinrich-Heine-Universität Düsseldorf,
Universitätsstraße 1, 40225 Düsseldorf, Germany*

Different computational techniques in combination with molecular dynamics computer simulation are used to determine the wall-liquid and the wall-crystal interfacial free energies of a modified Lennard-Jones (LJ) system in contact with a solid wall. Two different kinds of solid walls are considered: a flat structureless wall and a structured wall consisting of an ideal crystal with the particles rigidly attached to fcc lattice sites. Interfacial free energies are determined by a thermodynamic integration scheme, the anisotropy of the pressure tensor, the non-equilibrium work method based on Bennett acceptance criteria, and a method using Cahn’s adsorption equations based on the interfacial thermodynamics of Gibbs. For the flat wall, interfacial free energies as a function of different densities of the LJ liquid and as a function of temperature along the coexistence curve are calculated. In case of a structured wall, the interaction strength between the wall and the LJ system and the lattice constant of the structured wall are varied. Using the values of the wall-liquid and wall-crystal interfacial energies along with the value for the crystal-liquid interfacial free energy determined previously for the same system by the “cleaving potential method”, we obtain the contact angle as a function of various parameters; in particular the conditions are found under which partial wetting occurs.

I. INTRODUCTION

Interfacial free energies between a crystal or liquid in contact with a solid wall are a key determinant of several interfacial phenomena such as wetting [1], adhesion and heterogeneous nucleation [2–4]. However, they are difficult to determine in experiments and very few results are available in the literature (see e.g. [5–7]). Therefore, molecular simulation techniques such as Molecular Dynamics (MD) and Monte Carlo (MC) [8–10] play an important role to elucidate interfacial phenomena. Since molecular simulations can be used to determine the same thermodynamic quantity via various computational strategies, reliable estimates of the desired quantities are obtained by comparing the results obtained from the different methods. In this work, our objective is to employ several different computational techniques for obtaining reliable estimates of the wall-liquid and wall-crystal interfacial free energies, in the following denoted by γ_{wl} and γ_{wc} , respectively.

In order to calculate γ_{wl} , mechanical techniques can be employed to compute the interfacial tension from the pressure anisotropy (PA) [11]. Several authors have used this technique to calculate γ_{wl} for both hard-sphere [12–14] and Lennard-Jones (LJ) systems [15–21]. Since, in general, the interfacial tension is not equal to the interfacial free energy [22], except in case of a liquid in contact with a static wall, the mechanical approach fails in situations involving liquid in contact with a wall consisting of a “fully interacting solid phase” [23] or for a crystal in contact with a solid wall [24]. Another drawback is the massive computational effort needed to obtain reliable results, since the interfacial tension being the difference of the normal and tangential pressure profiles is very sensitive to small numerical errors [25, 26].

In contrast to the PA method, thermodynamic inte-

gration (TI) techniques [10, 31] are applicable to a wider class of systems including systems where the liquid interacts with an elastic wall or for wall-crystal interfaces. Various TI schemes have been proposed for the calculation of γ_{wl} and γ_{wc} and applied to systems modelled by hard-sphere, LJ or other soft interaction potentials [27–31]. While the TI method is simple to understand and easy to implement in MD or MC simulations, care has to be taken that the switching protocol that transforms the initial to the final state is reversible and does not lead to any hysteresis. As a result, the computational load can be considerable.

A less computationally expensive method, which does not require the constraint of a reversible switching protocol, is the non-equilibrium work method. In 1997, Jarzynski showed that one can extract the equilibrium free energy difference between two states from an exponential average of the non-equilibrium work performed on the system during a transformation from one state to another [32]. However, to obtain an accurate estimate of the free energy difference using the Jarzynski equality (JE), the tail of the work probability distribution must be well sampled, which is possible only if an extremely large number of independent runs are performed [33]. Therefore, in general, a direct application of the Jarzynski equality leads to a significant bias and variance in the free energy estimates [34]. Shirts *et al.* [35] demonstrated that one can overcome this disadvantage by carrying out both forward and backward transformations between the two states and then estimating the equilibrium free energy difference using the Bennett acceptance ratio (BAR) [36]. The BAR method has been applied to obtain the crystal-liquid interfacial free energy for both hard sphere and LJ systems [37, 38]. However, to the best of our knowledge there have been no studies where non-equilibrium work approaches have been used to compute

γ_{wl} or γ_{wc} .

If interfacial free energies are needed at many points along a coexistence curve, say, the TI and BAR methods would both be computationally expensive. Recently, Laird and others have obtained γ_{wl} for a hard-sphere system by integrating along a pressure curve [23] and the crystal-liquid interfacial free energy for LJ systems as a function of temperature along the coexistence curve [39] using the ‘‘Gibbs-Cahn integration’’ method. This technique is based on adsorption equations derived by Cahn [40] to extend Gibbs’s interfacial thermodynamics [41]. The ‘‘Gibbs-Cahn integration’’ (GC) method requires that the values for the interfacial free energy is already known at one point along the curve, then at the remaining points the free energies can be determined by integrating along the curve. While, Laird and Davidchack computed γ_{wl} for hard spheres in contact with a hard wall, there have been no corresponding studies for LJ systems.

Although, the above described methods can be employed to determine γ_{wl} and γ_{wc} , *a priori* it is not known which technique yields the most accurate results. To investigate this issue, we use different computational methods to arrive at reliable estimates for γ_{wl} and γ_{wc} and also discuss the computational efficiency of each method. To this end, we compute γ_{wc} and γ_{wl} for a LJ system in contact with solid walls from non-equilibrium work measurements using the JE and BAR methods and compare the results with a TI scheme devised in our earlier work [31]. The interfacial free energies are computed for both a bulk LJ liquid and a bulk LJ face centred cubic crystal oriented along the (111) direction. We consider two kinds of solid walls: one is a flat structureless wall and the other one is a structured wall consisting of particles rigidly attached to fcc lattice sites with the (111) orientation of the wall in contact with the system. In this work, γ_{wl} and γ_{wc} are obtained by our TI scheme and non-equilibrium work methods; the wall-liquid interfacial free energy, γ_{wl} is also determined via the GC method as well as the PA technique. Results from the four different approaches are compared with each other.

If in addition to the wall-liquid and wall-crystal interfacial free energies, one has knowledge about the crystal-liquid interfacial free energy, γ_{cl} , a direct determination of the degree of wetting of a solid surface by a substance can be obtained from Young’s equation [42],

$$\gamma_{wc} + \gamma_{cl} \cos \theta_c = \gamma_{wl} \quad (1)$$

with θ_c the contact angle. The contact angle controls whether crystal nucleation from the bulk liquid occurs preferably via homogeneous nucleation corresponding to complete drying ($\theta_c = 180^\circ$) or at the wall via heterogeneous nucleation corresponding to partial wetting ($0^\circ < \theta_c < 90^\circ$) or partial drying ($90^\circ < \theta < 180^\circ$) scenarios. However, to obtain θ_c from Eq. (1), the value for γ_{cl} is also needed. Therefore, we carried out simulations using a form of the LJ potential first introduced by Broughton and Gilmer [39, 43–46], for which γ_{cl} has

already been determined using the ‘‘cleaving potential’’ approach [44] as well as the Gibbs Cahn integration technique [39].

In the following, we introduce the details of the model potentials considered in this work (Sec. II), then describe the non-equilibrium work method and the Gibbs Cahn integration technique (Sec. III) and provide the main details of the simulation (Sec. III C). Then, we present the results (Sec. IV) and finally draw some conclusions (Sec. V).

II. MODEL POTENTIAL

We consider a system consisting of N identical particles, each of mass m , interacting with each other via a LJ potential first introduced by Broughton and Gilmer [43]. For two particles i and j separated by a distance r , this interaction potential is defined by

$$u(r) = \begin{cases} \phi(r) + C_1 & \text{for } 0 < r \leq 2.3\sigma \\ C_2 \left(\frac{\sigma}{r}\right)^{12} + C_3 \left(\frac{\sigma}{r}\right)^6 & \text{for } 2.3\sigma < r < 2.5\sigma \\ 0 & \text{for } r > r^c \end{cases} \quad (2)$$

with

$$\phi(r) = 4\epsilon \left[\left(\frac{\sigma}{r}\right)^{12} - \left(\frac{\sigma}{r}\right)^6 \right]. \quad (3)$$

In the following, energies and lengths are given in units of the parameters ϵ and σ , respectively. The cut-off distance r^c is set to $r^c = 2.5\sigma$. The constants in Eq. (2) are given by $C_1 = 0.016132\epsilon$, $C_2 = 3136.6\epsilon$, $C_3 = -68.069\epsilon$, $C_4 = -0.083312\epsilon$, and $C_5 = 0.74689\epsilon$.

To model the interaction of the LJ system with the structured wall we choose the purely repulsive Weeks-Chandler-Andersen (WCA) potential,

$$u_{sw}(r) = 4\epsilon_{sw} \left[\left(\frac{\sigma_{sw}}{r}\right)^{12} - \left(\frac{\sigma_{sw}}{r}\right)^6 + \frac{1}{4} \right] \quad (4)$$

for $0 < r \leq 2^{1/6}\sigma_{sw}$ and 0 otherwise where σ_{sw} is set to $\sigma_{sw} = 0.941\sigma$. Here, r represents the distance between a LJ particle in the bulk and a wall particle. The structured wall was constructed from an ideal fcc crystal with the (111) orientation along the z direction and with an integer number of unit cells that fit exactly into the simulation cell. The reason for choosing $u_{sw}(r)$ different from $u(r)$ was to obtain a large parameter range with respect to the energy scale ϵ_{sw} and the lattice constant of the wall a_{sw} [where $a_{sw} = (4/\rho_{sw})^{(1/3)}$, ρ_{sw} being the density of the structured wall], providing the possibility of incomplete wetting conditions. In the case of $u_{sw}(r) = u(r)$, complete wetting would be more likely than partial wetting, even for moderate interaction strengths between the wall and the LJ system.

The N identical LJ particles are enclosed within a simulation cell of size $L_x \times L_y \times L_z$, with periodic boundary

conditions in the x and y directions. Our simulations are carried out in the NVT ensemble with the total density $\rho = N/V$ kept constant. Along the z direction the particles are confined by the walls such that there are two planar wall-liquid (or wall-crystal) interfaces with a total area of $A = 2L_x L_y$ and with the Gibbs dividing surface located at the surface of the wall. The width of the structured wall is chosen large enough to avoid LJ particles on opposite sides of the wall from interacting with each other since the determination of interfacial free energy is built on the assumption of two independent wall-liquid (or wall-crystal) interfaces.

In our earlier work [31] on computing γ_{wl} and γ_{wc} for structured walls via TI, we adopted a scheme which consists of two steps. First, a bulk LJ system with periodic boundary conditions is transformed into a state where the LJ system is in contact with flat walls on either side in the z direction. Then, in the second step, the flat walls are reversibly transformed into structured walls. The structureless flat wall (fw) was also taken to be a purely repulsive potential interacting along the z direction with the LJ particles and is described by a WCA potential,

$$u_{fw}(z) = 4\epsilon \left[\left(\frac{\sigma}{z}\right)^{12} - \left(\frac{\sigma}{z}\right)^6 + \frac{1}{4} \right] \times w(z) \quad (5)$$

for $0 < z \leq z_{cw} = 2^{1/6}\sigma$ and zero otherwise. Note that for $u_{fw}(z)$ the parameters ϵ and σ are identical to those chosen for $u(r)$. The variable $z = z_i - Z$ denotes the distance between a particle i at z_i to one of the flat walls at $Z = z_b$ or $Z = z_t$. The function $w(z)$ ensures that $u_{fw}(z)$ goes smoothly to zero at $z = z_{cw}$ and is given by

$$w(z) = \frac{(z - z_{cw})^4}{h^4 + (z - z_{cw})^4}, \quad (6)$$

with the dimensionless parameter $h = 0.005$. Below, results for γ_{wl} and γ_{wc} for both the flat and structured wall cases are presented.

III. METHODS

When a system is transformed from one equilibrium state to another, the total work $\langle W \rangle$ performed on the system is larger than the free energy difference, ΔF , between the states,

$$\langle W \rangle \geq \Delta F. \quad (7)$$

This inequality holds because some of the work is always dissipated as heat, i.e.

$$\langle W^{\text{diss}} \rangle = \langle W \rangle - \Delta F \geq 0 \quad (8)$$

with W^{diss} the dissipated work. The equality $\langle W \rangle = \Delta F$ holds when the process is reversible such that the dissipated work goes to zero. This reversible work is essentially what one computes in the TI method where one

changes the switching parameter infinitely slowly such that the transformation is reversible. As a result, the TI method yields the free energy difference between a desired state and some reference state [10]. Usually a parameter which couples to the interaction potential is gradually changed such that the reference state is reversibly transformed into the final state of interest.

To calculate the interfacial free energy of the LJ system in contact with a structured wall, the TI scheme is carried out in two steps. In the first step, a bulk LJ system without walls and periodic boundary conditions in all directions is reversibly transformed into a LJ system in contact with a structureless flat wall along the z direction. In the second step, the flat wall interacting with the LJ system is reversibly transformed into a structured wall. Calculating the total free energy difference ΔF combined from the two steps yields the required interfacial free energy, defined as

$$\gamma = \frac{F_{\text{system}} - F_{\text{bulk}}}{A} = \frac{\Delta F}{A} \quad (9)$$

with F_{system} and F_{bulk} representing the Helmholtz free energies of the inhomogeneous system and the bulk phase of the system, respectively. For details we refer the reader to our earlier work [31]. In both steps of our TI scheme the transformation from one equilibrium state to another is carried out by gradually changing a switching parameter λ , which couples directly to the interaction potential.

Although the TI method yields reliable values for interfacial free energies, it is computationally expensive so as to ensure reversibility. In principle, the switching protocol needs to be infinitely slow when computing the free energy difference from a sequential change of the switching parameter or by carrying out simultaneous simulations at many independent values of the switching parameter between the initial and final states, so as to prevent any hysteresis or numerical integration errors resulting from a non-smooth thermodynamic integrand. Besides, in many cases a reversible TI path might be difficult to construct. A less computationally expensive method, which is independent of the reversibility of the switching protocol is the non-equilibrium work method.

A. γ from non-equilibrium work methods.

Equation (7) shows that the free energy difference between two equilibrium states can only be obtained from a reversible transformation between them. However, in 1997 Jarzynski [32] proposed an equality, now known as the Jarzynski equality, that allows to extract free energy differences between two states even if the transformation from the initial to the final state proceeds via a non-equilibrium process.

The Jarzynski equality (JE) can be written as

$$\langle \exp(-\beta W) \rangle = \exp(-\beta \Delta F) \quad (10)$$

with $\beta = 1/(k_B T)$ (k_B : Boltzmann constant, T : temperature) and the work

$$W = \int_{t=0}^{t_s} \frac{\partial H(\lambda)}{\partial \lambda} \dot{\lambda} dt. \quad (11)$$

Here, the Hamiltonian $H(\lambda)$ [see Eq. (7) of Ref. [31] and accompanying text for details regarding the Hamiltonian] depends on the parameter λ that provides the switching from state to state; $\dot{\lambda}$ is the rate at which the parameter λ is changed to transform one state to another. The integration in Eq. (11) starts from an equilibrium state at time $t = 0$ to a final state at the switching time $t = t_s$. In a simulation, the free energy difference between the initial and the final state is estimated by

$$\Delta F_{\text{JE}} = -k_B T \ln \sum_{i=1}^{N_{\text{runs}}} \exp(-\beta W_i) \quad (12)$$

with N_{runs} the number of independent runs and W_i the value of the work, obtained from the i 'th run. The estimate ΔF_{JE} approaches the exact free energy difference ΔF for $N_{\text{runs}} \rightarrow \infty$.

For slow transformations ($t_s \rightarrow \infty$), the system is in quasi static equilibrium at each instant throughout the transformation and the switching process reduces to a conventional TI. However, for finite switching times t_s , the system is in a non-equilibrium state and while the JE holds irrespective of the duration t_s over which the switching parameter is varied, its practical utility is limited since the exponential work average depends on how well the tail of the work probability distribution with work values that are less than the equilibrium free energy difference are sampled [33]. As a result, the JE is a practical tool to obtain free energy differences only for slow switching processes where the system remains close to equilibrium at each instant during the transformation. In such a situation, the average work converges to ΔF within a reasonable number of independent runs. However, for fast switching times, the exponentially averaged work exhibits a huge bias in comparison to the equilibrium free energy difference and is also accompanied by a large standard deviation [34].

Shirts *et al.* [35] showed that a good convergence toward ΔF can be obtained by carrying out simulations with both forward as well as reverse switching runs. In the reverse runs, the final state is transformed into the initial state by following a mirror image of the forward switching protocol. Using the Bennett acceptance ratio (BAR) method [36], the free energy difference is finally obtained from the following transcendental equation,

$$\sum_{i=1}^{N_F} \frac{1}{1 + \exp[\frac{W - \Delta F}{k_B T}]} - \sum_{i=1}^{N_R} \frac{1}{1 + \exp[-\frac{W - \Delta F}{k_B T}]} = 0 \quad (13)$$

that can be solved via the Newton-Raphson method [47]. In Eq. (13), F and R represent respectively the forward

and reverse switching processes and N_F and N_R refer respectively to the number of forward and reverse switching trajectories. For simplicity, we consider the case $N_F = N_R$. It has been shown that the BAR method leads to the minimum bias and variance when computing the free energy difference via non-equilibrium work methods [35].

The efficiency of the BAR method crucially depends on the switching time t_s used to transform the initial state to the final state. A large switching time will make the method inefficient, while an extremely short t_s will lead to a bias in the free energy estimate. The optimal switching time is not known beforehand. Hence, we will use both the JE and BAR methods with the same parametrization as in the TI scheme and with three different switching times ($t_s = 5, 50$ and 500 in reduced units) to compute the interfacial free energies and compare our results to the TI method.

Corresponding to the first step in the TI, the forward switching process transforms the bulk LJ system into that in contact with impenetrable flat walls in the z direction. For this step the reverse process consists of gradually switching off of the flat walls in contact with the system to revert back to the bulk liquid or crystal with periodic boundary condition in all directions. Similarly, corresponding to the second TI step, the forward switching process consists of a LJ system in contact with a flat wall being transformed to one in contact with the structured wall. In the reverse process, the structured walls are gradually switched off and the flat walls switched on, such that a liquid or crystal in contact only with a flat wall is obtained as the final state.

B. γ from Gibbs-Cahn integration

While the non-equilibrium work method might be computationally advantageous compared to the TI scheme, it is still inefficient if one needs to compute the interfacial free energies at many points along a coexistence curve. Carrying out simulations at each point would be cumbersome and require a huge computational effort. In such cases it is computationally advantageous to use the ‘‘Gibbs-Cahn integration’’ method, where a differential equation is solved to obtain interfacial free energies along a coexistence curve if the value at one point on the curve is known beforehand from the TI or BAR method.

The Gibbs-Cahn integration method has been used to obtain the interfacial free energy of a hard-sphere fluid in contact with a flat wall [23], the crystal-liquid interfacial free energy for LJ systems [39], and the crystal-vapor and crystal-liquid interfacial free energies for metallic systems [48, 49]. In this work, Gibbs-Cahn integration is used to compute, for a flat wall, the wall-liquid free energy γ_{wl} along coexistence as well as along an isotherm varying the density of the liquid.

The Gibbs-Cahn differential equation for γ_{wl} along the pressure-temperature ($P - T$) coexistence curve is given

by [23]

$$d(\gamma/T) = -\frac{e_N + Pv_N}{T^2}dT + \frac{v_N}{T}dP, \quad (14)$$

with v_N the interfacial excess volume,

$$v_N = \int_0^\infty \left[1 - \frac{\rho(z)}{\rho} \right] dz, \quad (15)$$

and e_N the interfacial excess energy,

$$e_N = \rho e \int_0^\infty \left(\frac{e(z)}{e} - 1 \right) dz. \quad (16)$$

In Eqs. (15) and (16), ρ and e are the bulk density and the bulk energy per particle, respectively. $\rho(z)$ and $e(z)$ are respectively the corresponding density and energy profiles along the z direction, i.e. the direction perpendicular to the walls. If the value of γ_{wl} is known at any point along the coexistence curve by the TI or BAR method, Eq. (14) can be used to determine γ_{wl} at any other point along coexistence. Following the derivation of a GC integration equation for calculating γ_{cl} in Ref. [39], probably one can obtain a similar equation for computing γ_{wc} for a crystal in contact with a flat wall, though none exists in the literature. However, in this work we use the GC integration method only for calculating γ_{wl} .

The Gibbs-Cahn integration method is most useful when interfacial free energies are needed along a parameter space where an intensive thermodynamic variable such as pressure or temperature is varied. Since for structured wall interfaces we compute the interfacial free energies as a function of the wall density and interaction strength between the bulk phase and wall, the GC method is not suitable for such cases. Therefore, we use only the TI and BAR methods for computing the interfacial free energies for liquid or crystal in contact with a structured wall.

C. Simulations

Molecular dynamics (MD) computer simulations are performed at constant particle number N , constant volume V , and constant temperature T . To keep the temperature constant, the velocities of the particles were drawn from a Maxwell-Boltzmann distribution at the desired temperature every 200 time steps. The density $\rho = N/V$ of the crystal and liquid at coexistence, corresponding to the modified LJ potential considered in this work, were taken from Ref. [39]. As in our earlier work, only the (111) orientation of the LJ crystal was considered. To integrate the equations of motion, the velocity form of the Verlet algorithm was used with a time step of $\Delta t = 0.005\tau$ (with $\tau = \sqrt{m\sigma^2/\epsilon}$).

Since the simulations were performed in the NVT ensemble, it is expected that the bulk density would differ from the given density $\rho = N/V$ at which the simulations are carried out when walls are introduced, thereby

changing the pressure. To account for this, simulations were done at three to four different system sizes with respect to a variation of the distance between the walls, L_z , in z -direction, keeping the lateral dimensions ($L_x \times L_y$) constant. Interfacial free energies were obtained by extrapolating the results to $1/L_z = 0$. To reduce finite size effects, lateral sizes of about $12 - 16\sigma$ were considered and along the z direction the length of the simulation cell varied from about 30σ for the smallest system sizes to around 90σ for the largest system sizes. The smallest value of L_z considered was large enough to avoid any spurious effects due to interactions between the two wall-liquid (or crystal) interfaces. For the considered systems, the total number of particles varied from around $N = 7000$ to about $N = 18000$.

For the TI and BAR methods, periodic boundary conditions are employed along the x , y and z directions when the LJ system is in contact with flat walls since we transform a bulk LJ system periodic in all directions to a system in contact with impenetrable flat walls. In the second step, when the flat walls were transformed to structured walls, periodic boundary conditions are only used along the x and y directions. The GC and PA simulations are carried out with periodic boundary conditions only along the x and y directions.

For the simulations involving a flat wall, γ_{wl} was computed along an isotherm (at the temperature $T = 1.0$) at several densities upto the coexistence density of the liquid, $0.9288\sigma^{-3}$, using PA, TI, BAR and the GC integration methods. γ_{wl} was also computed as a function of temperature along the melting curve at five different temperatures, viz. $T = 0.618, 0.809, 1.0, 1.25,$ and 1.5 [note that $T = 0.618$ corresponds to the triple point temperature for the modified LJ potential, as given by Eq. (2)]. At the latter temperatures, the coexistence densities of the crystal are $0.9445\sigma^{-3}, 0.9744\sigma^{-3}, 1.0044\sigma^{-3}, 1.0411\sigma^{-3}$ and $1.0743\sigma^{-3}$ from the lowest to the highest temperature, respectively. The corresponding coexistence densities for the liquid phase are $0.8282\sigma^{-3}, 0.8829\sigma^{-3}, 0.9288\sigma^{-3}, 0.9644\sigma^{-3},$ and $1.0030\sigma^{-3}$, respectively. These coexistence densities were taken from the work of Laird *et al.* [39], who determined the crystal-liquid interfacial free energy for the same potential using the GC [39] and the ‘‘cleaving potential’’ approach [44]. The interfacial free energy γ_{wc} was computed at the indicated five different temperatures along the coexistence curve using only the BAR and TI methods.

The statistical error bars for the TI method were calculated from 5 different sets of data with each data set representing an average over 10000 configurations. For the non-equilibrium work simulations, the free energy difference was obtained from 3 or 4 different data sets with each data set representing an average over 3 or 4 independent trajectories. In each of the figures the error bars represent one standard deviation away from the mean.

The data for GC and PA were calculated from 3 – 4 independent realizations, with each realization representing an average over two million configurations. While

averaging over such a large number of independent configurations is not needed for obtaining the interfacial excess quantities used in the GC integration method, it is necessary for computing the pressure profiles with high precision when computing interfacial free energies via the PA method as the interfacial free energy being the difference between the normal and tangential pressure profiles is very sensitive to small numerical errors in the pressure profiles [26]. For the GC and PA data, the error bars for the interfacial excess quantities (e_N and v_N) as well as γ_{wl} correspond to one standard deviation away from the mean.

As is clear from Eq. (14), the bulk pressures must also be calculated at each temperature or density to compute the integrals. Since we carry out simulations in the NVT ensemble, the bulk pressures would be different for different system sizes along the z direction. Hence, we calculated the bulk pressures, performed the integration at each system size, and then extrapolated the results to $1/L_z = 0$. To compute the interfacial excess energy and the interfacial excess volume for use in the GC integration method, a bulk region must be identified in the middle of the simulation cell and away from the walls. We choose a length of 5σ in the middle of the simulation cell to calculate the bulk density, pressure and energy per particle and the same length was considered for all system sizes. To calculate the density, pressure and energy profiles a bin size of 0.05σ was chosen along the z direction. All integrals in the TI method as well as the GC integration method were performed by the trapezoidal rule and it was checked that numerical integration errors were less than the statistical errors.

IV. RESULTS

For a direct comparison of the TI, PA, GC and BAR methods, we computed γ_{wl} for the case of a liquid in contact with a flat wall. Since the PA method and probably also the GC approach cannot be used to compute γ_{wc} , this quantity is only determined via the TI and BAR methods. In the following, different wetting conditions are mainly studied for one state at coexistence, corresponding to the temperature $T = 1.0$ and the crystal and liquid coexistence densities at $1.0044 \sigma^{-3}$ and $0.9288 \sigma^{-3}$, respectively. For this case, γ_{wl} and γ_{wc} are investigated as a function of the interaction parameters ϵ_{sw} and ρ_{sw} . Note that for the structured wall only the TI and BAR methods are employed. We first present the results corresponding to the interfaces with the flat wall and then discuss the case of the structured wall.

A. Flat wall

We first show results obtained from the four different methods at temperature $T = 1.0$ and the coexistence densities $0.9288 \sigma^{-3}$ and $1.0044 \sigma^{-3}$ for the liquid and

the crystal, respectively. In the following, we denote the estimated interfacial free energy from JE [cf. Eq. (12)] for the forward switching process by ΔF_{JEF} and that for the negative of the reverse switching process by $-\Delta F_{JER}$. We compare ΔF_{JEF} and $-\Delta F_{JER}$ to the correspondent average work values (divided by the interface area A), $\langle W \rangle_F/A$ and $-\langle W \rangle_R/A$, respectively. Estimates of γ_{wl} and γ_{wc} from the non-equilibrium work methods as a function of switching time t_s are shown in Figs. 1 and 2, respectively. Note that all the results in these figures are obtained from an extrapolation to $L_z^{-1} = 0$ (see above). Since, $\langle W \rangle_F > \Delta F$, it follows that $\langle W \rangle_R > -\Delta F$ or $-\langle W \rangle_R < \Delta F$. These relations are rationalized by our calculations (see figures).

Figures 1 and 2 show that, as the switching time t_s increases, ΔF_{JEF} and $-\Delta F_{JER}$ gradually converge to the interfacial free energies, as obtained from the TI scheme (horizontal dotted lines). As indicated in the figures, the JE values are similar to the corresponding average work values. Whereas at small switching times ($t_s \lesssim 50$) the JE estimates significantly differ from the TI value, for $t_s = 500$ the deviation between the JE and TI values is less than 2% (this also holds for the corresponding average work values). On the other hand, the free energy estimated by the BAR method is in excellent agreement with the TI value already at $t_s = 50$, with difference between the two estimates being less than 0.3%. However, at $t_s = 50$, the error bars corresponding to the BAR method are larger than those of the TI values. Only at $t_s = 500$, the error bars for the BAR and TI method have the same order of magnitude. Similarly, the magnitude of the error bars corresponding to the JE estimates and the average work values reduce to those of the TI method at $t_s = 500$.

We find that the BAR method (with $t_s = 50$) is twice

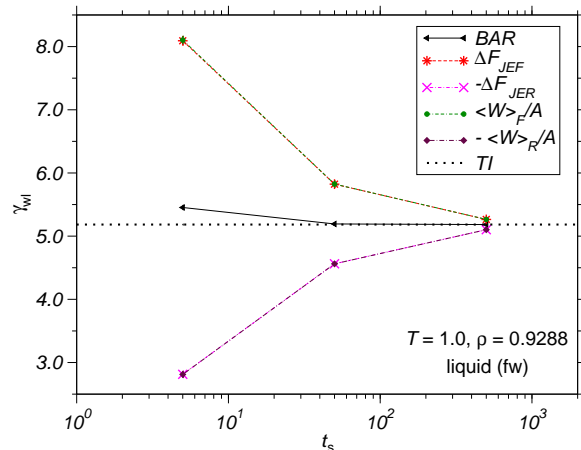


FIG. 1: (Color online) Estimates of γ_{wl} for the flat wall (fw) at the indicated values of T and ρ from non-equilibrium work methods (see text). The horizontal dotted line is the result from TI. All results are obtained from an extrapolation to $L_z^{-1} = 0$. Error bars are not shown as they are less than the symbol size.

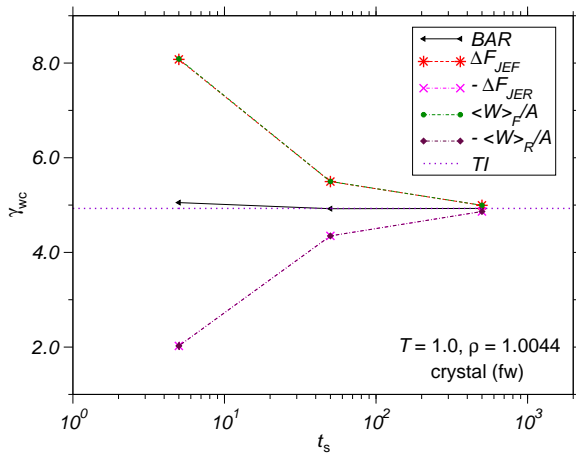


FIG. 2: (Color online) γ_{wc} vs. t_s at the indicated values of T and ρ obtained using TI and several non-equilibrium work methods. Error bars are less than the symbol size.

as fast as the TI approach, though, for $t_s = 50$, the error bars for the BAR method are slightly larger. At $t_s = 500$, the error bars and also the computational load for the BAR and the TI method are similar and the BAR method is no more computationally advantageous compared to the TI approach. On the other hand, the computational load needed for the JE estimates and the corresponding average work values, at $t_s = 500$, is about one third that of the TI method, which is still faster compared to the BAR method at the smaller switching time $t_s = 50$. Since the BAR approach requires information from both the forward and reverse trajectories its efficiency is reduced as compared to the JE estimates, which need calculations only in one direction, either forward or reverse.

The good agreement of the average work values for $t_s = 500$ with the TI results, shows that at this switching time the switching process is quasi-static and hence is akin to a TI. In our TI simulations, carried out independently of the non-equilibrium work simulations, we choose a much larger equilibration time before the production runs thus increasing the computational load. Hence, an advantage of carrying out simulations with various switching times to calculate the non-equilibrium work, allows us to identify the switching time required for the transformation from the initial to the final state to be quasi-static and reduce to a conventional TI. The good agreement of the average work values with JE estimates at $t_s = 500$ and with the TI data also indicates that there is no advantage in using the non-equilibrium work method over a TI approach as regards computational speed is concerned. However, carrying out simulations for both forward and reverse switching processes help us to check for any hysteresis in the TI. The convergence of both the forward and reverse work values (divided by A) to the interfacial free energy obtained from TI, indicates the lack of hysteresis in our TI scheme. Secondly, the good agreement between the non-equilibrium work and TI method also validates the accuracy of our

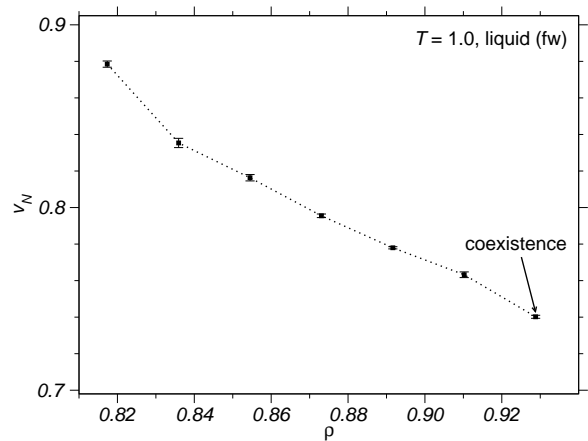


FIG. 3: (Color online) Excess interfacial volume v_N as a function of density at $T = 1.0$, for the liquid in contact with a flat wall (fw).

TI method.

In the remainder of this subsection, unless otherwise indicated, we show results pertaining to the non-equilibrium work approach obtained using only the BAR method for the switching time $t_s = 500$.

To determine the interfacial free energy along an isotherm at different densities or along a coexistence curve at different temperatures via the GC integration we need as input γ_{wl} at one point along the curve as well as the excess volume (in case of determining γ_{wl} along the coexistence curve, also the excess energy) at all points along the curve at which γ_{wl} is to be determined.

Figure 3 shows the excess volume as a function of density up to the coexistence density at $T = 1.0$. Since the temperature is constant ($dT = 0$), the first term in Eq. (14) is zero and we only need the interfacial excess volume, $v_N(\rho)$ and one reference value for γ_{wl} . Here,

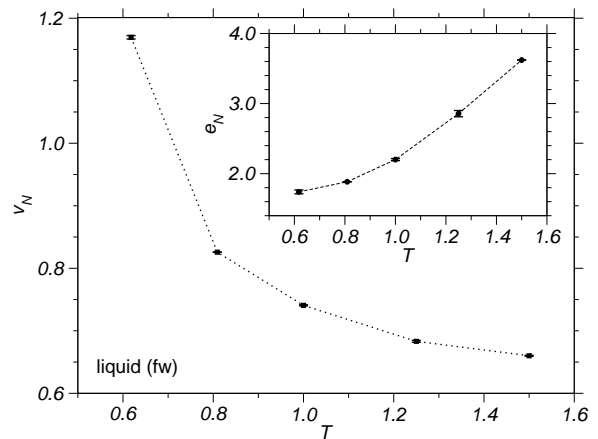


FIG. 4: (Color online) Excess interfacial volume v_N and (in the inset) excess interfacial energy (e_N) as a function of the temperature along the liquid-crystal coexistence curve for liquid in contact with a flat wall.

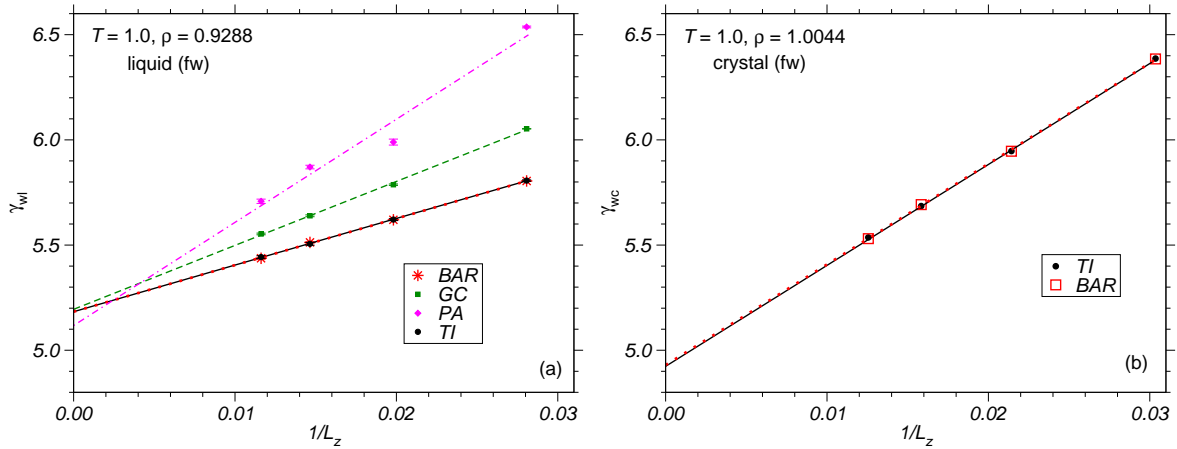


FIG. 5: (Color online) Interfacial free energies of the (a) liquid in contact with the flat wall and (b) (111) orientation of the crystal in contact with the flat wall for different system sizes L_z of the simulation cell along the z direction at the coexistence temperature $T = 1.0$. The coexistence densities of the liquid and crystal at this temperature are $0.9288\sigma^{-3}$ and $1.0044\sigma^{-3}$ respectively. For the wall-liquid interfaces, the interfacial free energy obtained from the PA, GC, TI and BAR methods are shown, while for the wall-crystal simulations, data obtained from the TI and BAR methods are plotted. The straight lines connecting the points denote a linear least-squares fit from whose intercepts the interfacial free energies are determined. In (b) error bars are less than the symbol size.

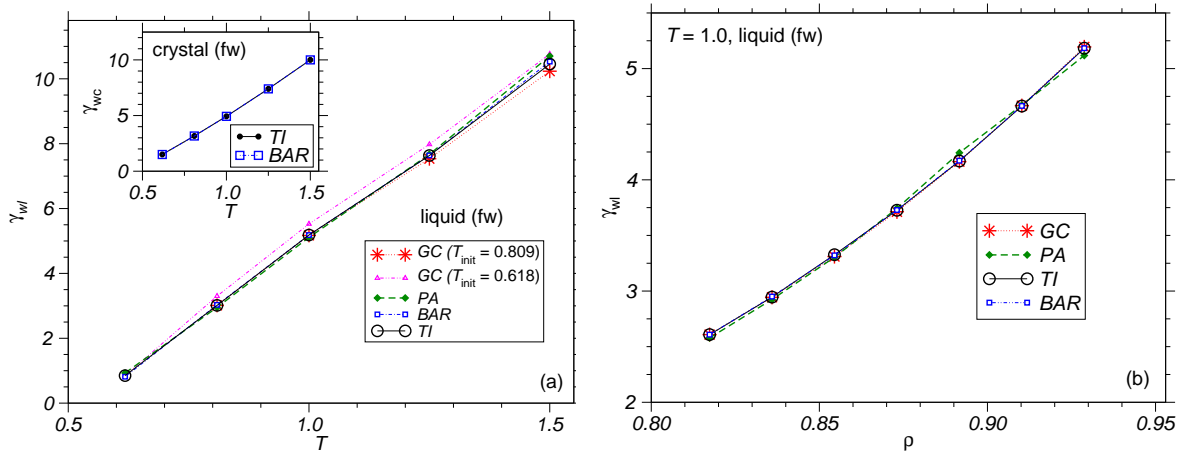


FIG. 6: (Color online) (a) γ_{wl} and γ_{wc} (shown in the inset) as a function of the melting temperature and (b) γ_{wl} vs. density of the liquid at $T = 1.0$. In (a) two sets of GC data are shown for γ_{wl} . One corresponds to data where the initial known value of the interfacial free energy is taken from the TI data at $T = 0.618$ and the values for $T > 0.618$ obtained via GC integration. The second curve corresponds to the case where the known value of γ_{wl} was taken from the TI data at $T = 0.809$ and for $T > 0.809$, the interfacial free energies are obtained using GC integration. In case of (b), the known value of γ_{wl} was taken from the TI data at the lowest value of the given liquid density. The data corresponding to the BAR method represent results for a switching time $t_s = 500.0$. Error bars in (a) and (b) are less than the symbol size.

this reference value was taken from the TI result corresponding to the lowest density at $\rho_l = 0.811\sigma^{-3}$. Note that the lateral system sizes were kept at $L_x = 13.5892\sigma$ and $L_y = 15.691\sigma$ for the different densities. From the lowest to the highest density, the system sizes along the z direction were 66.907σ , 65.420σ , 63.998σ , 62.636σ , 61.331σ , 69.678σ , and 68.285σ , respectively. The number of particles for all densities up to $\rho_l = 0.8916\sigma^{-3}$ was $N = 11661$. For $\rho_l = 0.9102\sigma^{-3}$ and $\rho_l = 0.9288\sigma^{-3}$,

$N = 13524$ was chosen.

The interfacial excess quantities were also computed for all the other system sizes from which the final value of γ_{wl} was determined by an extrapolation to $L_z^{-1} = 0$. At all other system sizes, the interfacial excess quantities had similar values and varied in the same manner along the isotherm at the different densities. There was no clear dependence of the interfacial excess quantities on the system size. As the density increases and approaches the liq-

uid coexistence density at this temperature, $0.9288 \sigma^{-3}$, the bulk pressures in the liquid also increase. Similar to the hard-sphere case [39], we also find that the excess volume decreases with increasing density (or bulk pressure).

Figure 4 shows the excess volume and excess energy as function of temperature at coexistence. The system sizes $L_x \times L_y \times L_z$ corresponding to the different temperatures are as follows: $13.871 \times 16.016 \times 63.378$ at $T = 0.618$, $13.727 \times 15.851 \times 70.397$ at $T = 0.809$, $13.589 \times 15.691 \times 68.285$ at $T = 1.0$, $13.428 \times 15.505 \times 67.357$ at $T = 1.25$, and $13.288 \times 15.344 \times 66.134$ at $T = 1.5$ (with all lengths in units of σ). The number of particles was $N = 11661$ at $T = 0.618$ and $N = 13524$ at the other temperatures. It is observed that the excess volume decreases with temperature while the excess energy shows an increase with temperature. We note that the interfacial excess quantities do not exhibit finite-size effects for the considered system sizes.

For each individual run and system size, the interfacial excess quantities and the GC integration was carried out independently to obtain γ_{wl} along an isotherm as a function of density and along the melting curve as a function of temperature. From the obtained values of γ_{wl} for the four considered system sizes, an extrapolation was performed to $L_z^{-1} = 0$ and the final values were calculated from the intercepts with the ordinate. In Figs. 5a and 5b, we show the results for the interfacial free energy from the various methods as a function of $1/L_z$ for the liquid and crystal in contact with the flat wall, respectively. While the extrapolated values obtained from the BAR, TI and GC methods are in good agreement with each other up to the numerical accuracy, results obtained from the PA method deviate from the rest by 2 – 3%.

Figure 6a shows γ_{wc} and γ_{wl} as a function of temper-

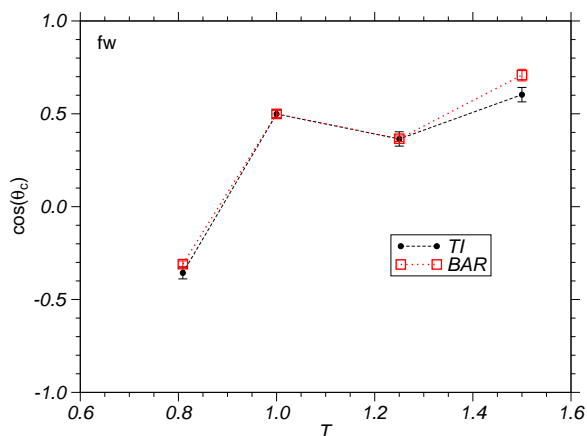


FIG. 7: (Color online) Cosine of the contact angle as a function of temperature along liquid-crystal coexistence for system in contact with a flat wall, obtained from Young's equation by using γ_{wl} and γ_{wc} from the TI and BAR data of Fig. 6a and using values of γ_{cl} as reported in Ref. [44]. Error bars are less than the symbol size.

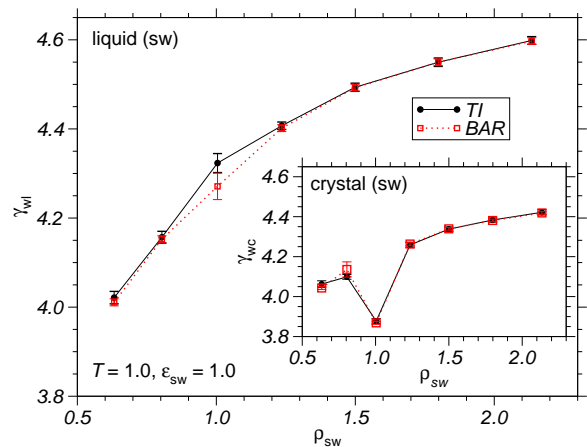


FIG. 8: (Color online) γ_{wl} and γ_{wc} (shown in the inset) as function of ρ_{sw} at the temperature $T = 1.0$ and $\epsilon_{sw} = 1.0$, obtained from the BAR (with $t_s = 500$) and the TI method.

ature along the melting curve, and in Fig. 6b, γ_{wl} is displayed as a function of density at $T = 1.0$. For the crystal, we find very good agreement between the BAR and the TI methods (inset of Fig. 6). To determine γ_{wl} along the melting curve, the interfacial free energy obtained from the TI method at $T = 0.618$ was first chosen as the initial value for the GC integration. With this initial value, the agreement of the GC integration data with the TI and BAR data becomes progressively worse with temperature and at $T = 1.5$, the difference between GC and TI or BAR result is around 9%. However, when the value of γ_{wl} obtained from TI at $T = 0.809$ is taken as the initial value, the agreement between the different methods is much better. This could be attributed to the fact that the pressure-temperature melting curve for LJ potentials that we consider here is clearly non-linear [46] between $T = 0.618$ and $T = 0.809$ signifying that more

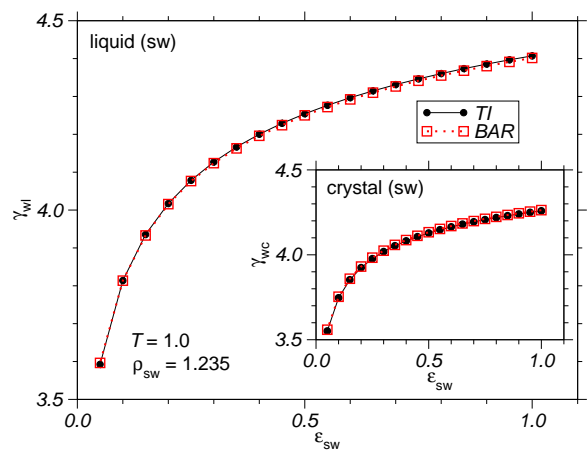


FIG. 9: (Color online) γ_{wl} and γ_{wc} (shown in the inset) versus the interaction strength ϵ_{sw} at the temperature $T = 1.0$ and $\rho_{sw} = 1.235$ obtained using the BAR (with $t_s = 50$) and TI methods. Error bars are less than symbol size.

data is needed between these two temperatures, whereas it exhibits essentially linear behavior for $T \geq 0.809$.

For the GC simulations to compute γ_{wl} along an isotherm at different densities, the interfacial free energy obtained from the TI method at the lowest density was chosen as the initial value to carry out the integration. Figure 6b clearly shows excellent agreement between all the four methods. The error bars corresponding to the different methods are all of a similar magnitude.

From the values for γ_{wl} and γ_{wc} predicted by the BAR and TI methods and using the data from Ref. [44] for γ_{cl} , we determined the cosine of the contact angle as a function of temperature along the coexistence curve via Young's equation. The results are shown in Fig. 7. At $T = 0.618$, $(\gamma_{wl} - \gamma_{wc})/\gamma_{cl} < -1$, corresponding to the complete drying conditions. As T increases, the flat wall prefers the crystal more than the liquid ($\gamma_{wc} < \gamma_{wl}$) and incomplete wetting is observed ($-1 < \cos \theta_c < 1$). At higher temperatures ($T > 1.0$) partial wetting is observed ($0 < \cos \theta_c < 1$), with $\cos \theta_c$ varying non-monotonically with respect to temperature along the melting curve. While good agreement is found in general between the BAR and TI methods, here, we observe a slightly larger difference between them as compared to that for the individual interfacial free energies. This is because $\cos \theta_c$ depends on the difference between γ_{wl} and γ_{wc} , which magnifies the relative error.

B. Structured Wall

We now consider the LJ system in contact with a structured wall, with the interaction between the wall and the LJ system to be of the same purely repulsive WCA potential. For the structured wall, the interesting parameters

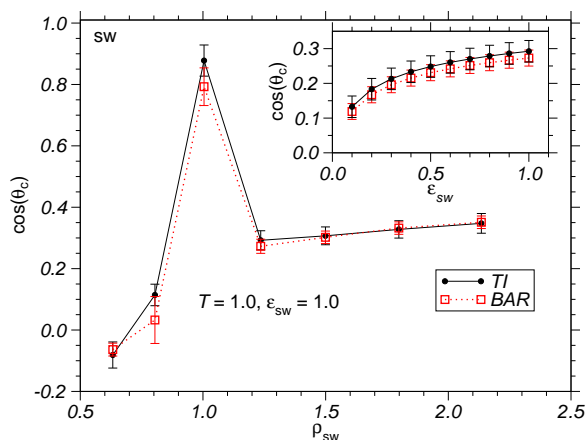


FIG. 10: (Color online) Cosine of the contact angle obtained from Young's equation at the temperature $T = 1.0$ as a function of ρ_{sw} at $\epsilon_{sw} = 1.0$ and in the inset versus the interaction strength ϵ_{sw} at $\rho_{sw} = 1.235$. γ_{wl} and γ_{wc} were taken from the BAR and TI data of Figs. 8 and 9 and values of γ_{cl} reported in Ref. [44] were used.

are the interaction strength and the density of the wall. We study the variation of the interfacial free energy as a function of these two parameters at the liquid-crystal coexistence temperature $T = 1.0$, choosing the coexistence densities $0.9288 \sigma^{-3}$ and $1.0044 \sigma^{-3}$ for the liquid and the crystal, respectively. In the following the BAR and the TI method are compared.

In Fig. 8, we plot the interfacial free energies of the LJ liquid and crystal as a function of the density of the wall (at $\epsilon_{sw} = 1.0$). In the computations with the BAR method a switching time of $t_s = 500$ was used. The density of the structured wall was modified by choosing different lattice constants for the fcc structure of the wall. We observe that the interfacial free energy of the liquid increases with increasing density of the wall. Increasing density of the wall means a larger repulsive force acting on the liquid particles which enhances γ_{wl} . The general trend for γ_{wc} is the same. However, when the density of the wall is the same as the equilibrium density of the crystal we find a sharp dip in the interfacial free energy. This is expected since when the wall has the same structure as the crystal less energy is required to create an interface.

Figure 9 shows γ_{wl} and γ_{ws} for different interaction strengths ϵ_{sw} between the wall and the LJ system. The density of the substrate is $\rho_{sw} = 1.235$, i.e. the density of the structured wall is larger than that of the bulk LJ crystal. To reduce the computational effort, ϵ_{sw} was itself used as the switching parameter, with the system at $\epsilon_{sw} = 1$ considered as the reference state. For the BAR calculations, a switching time $t_s = 50$ was sufficient to obtain good agreement with the TI method as regards the mean value and also the standard deviation. All the data corresponding to the BAR calculations in Fig. 9 are shown for a switching time $t_s = 50$. Increasing the interaction strength between the wall and the LJ system leads to a greater repulsive interaction between them, thereby enhancing the interfacial free energies.

As can be inferred from Figs. 8 and 9, at the considered thermodynamic states $\gamma_{wc} < \gamma_{wl}$ holds. This signifies the occurrence of incomplete wetting. To determine the contact angle from Young's equation, we use γ_{cl} , as obtained by the cleaving potential method [23], and γ_{wl} and γ_{wc} , as estimated by our TI scheme and the BAR method. Figure 10 shows that cosine of the contact angle increases with the density of the structured wall, with a sharp peak when the density of the wall is equal to the average density of the bulk crystal. At this value of the wall density, we found that the corresponding contact angle reaches a minimum and is about 25° , which is in the partial wetting regime. Contact angles are less than 90° ($0 < \cos \theta_c < 1$) at all wall densities except at the smallest ρ_{sw} since there $\gamma_{wc} > \gamma_{wl}$ (see Fig. 8).

Figure 10 also shows $\cos \theta_c$ increasing with increasing interaction strength between the the wall and the LJ system. This is because γ_{wl} and γ_{wc} gradually diverge from each other as ϵ_{sw} increases, as is clearly seen in Fig. 9. $0 < \cos \theta_c < 1$ at all values of ϵ_{sw} indicating that the LJ

crystal partially wets the wall for such parameter values.

V. CONCLUSION

In this work, extensive MD simulations of a LJ system were performed to compare different techniques for the calculation of wall-liquid and wall-crystal interfacial free energies. We find that the equilibrium thermodynamic integration (TI) method is in very good agreement with non-equilibrium work techniques such as the Bennett acceptance ratio (BAR) method. Within the restricted range of applicability, this also holds for Gibbs-Cahn (GC) integration and the pressure anisotropy (PI) method. This indicates the accuracy of the obtained estimates and also validates the TI scheme, proposed in our earlier work.

While the GC method is computationally faster compared to the TI or BAR methods, care has to be taken when the coexistence pressure and temperature vary nonlinearly along the melting curve since then more number of points are needed to obtain reliable values for the interfacial free energy. As a matter of fact, non-equilibrium work methods are not more efficient compared to conventional TI. However, such methods are helpful to check for any hysteresis in the TI scheme.

Using the obtained values of γ_{wl} and γ_{wc} and the values

for γ_{cl} calculated previously using the “cleaving potential method” [44], we applied Young’s equation to determine contact angles for flat and structured walls. In general, one observes smaller contact angles at higher temperatures along the melting curve when the LJ system is in contact with the flat wall. For the structured wall interfaces, it is found that the density of the structured wall and the interaction strength of the LJ particles with the wall significantly influence the contact angle and the degree of wetting can be changed by tuning such parameters. In particular, the contact angle exhibits a strongly non-monotonic behavior with respect to the density of the structured wall, as it shows a sharp minima when the density of the structured wall is equal to that of the bulk crystal.

Both for the flat and the structured walls we have obtained the conditions under which partial wetting is observed. Thus, the models proposed in this work can now be used for the study of heterogeneous nucleation.

Acknowledgments

We acknowledge support by the Deutsche Forschungsgemeinschaft (DFG) under Grant Nos. HO 2231/6-2 and HO 2231/6-3.

-
- [1] P. G. de Gennes, Rev. Mod. Phys. **57**, 827 (1985); P. G. de Gennes, F. Brochart-Wyart, and D. Quéré, *Capillarity and Wetting Phenomena. Drops, Bubbles, Pearls, Waves* (Springer, New York, 2004).
 - [2] A. C. Zettlemoyer (ed), *Nucleation* (New York: Dekker, 1969).
 - [3] F. F. Abraham, *Homogeneous Nucleation Theory* (New York: Academic, 1974).
 - [4] D. Kashchiev, *Nucleation: Basic Theory with Applications* (Oxford: Butterworth-Heinemann, 2000).
 - [5] A. W. Adamson and A. P. Gast, *Physical chemistry of surfaces* (Wiley-Interscience, New York, 1997).
 - [6] G. Navascués, Rep. Prog. Phys. **42**, 1131 (1979).
 - [7] J. M. Howe, *Interfaces in Materials* (Wiley, New York, 1997); M. E. Glicksman and N. B. Singh, J. Cryst. Growth **98**, 277 (1989); M. Muschol, D. Liu, and H. Z. Cummins, Phys. Rev. A **46**, 1038 (1992).
 - [8] M. P. Allen and D. J. Tildesley, *Computer Simulations of Liquids* (Clarendon, Oxford, 1987).
 - [9] D. P. Landau and K. Binder, *A Guide to Monte Carlo Simulations in Statistical Physics* (Cambridge, USA, 2000).
 - [10] D. Frenkel and B. Smit, *Understanding Molecular Simulation* (Academic, San Diego, 2002); T. P. Straatsma, M. Zacharias, and J. A. MacCammon, *Computer Simulations of Biomolecular Systems* (Escom, Keiden, 1993).
 - [11] J. G. Kirkwood and F. P. Buff, J. Chem. Phys. **17**, 338 (1949).
 - [12] J. R. Henderson and F. van Swol, Mol. Phys. **51**, 991 (1984).
 - [13] D. J. Courtemanche, T. A. Pasmore and F. van Swol, Mol. Phys. **80**, 861 (1993).
 - [14] E. De Miguel and G. Jackson, Mol. Phys. **104**, 3717 (2006).
 - [15] J. H. Sikkenk, J. M. J. van Leeuwen, J. O. Indekeu, J. M. J. van Leeuwen, E. O. Vossnack, and A. F. Bakker, J. Stat. Phys. **52**, 23 (1988).
 - [16] M. J. P. Nijmeijer, C. Bruin, A. F. Bakker, and J. M. J. Van Leeuwen, Physica A **160**, 166 (1989).
 - [17] M. J. P. Nijmeijer, C. Bruin, A. F. Bakker, and J. M. J. van Leeuwen, Phys. Rev. A **42**, 6052 (1990).
 - [18] M. J. P. Nijmeijer, C. Bruin, A. F. Bakker, and J. M. J. van Leeuwen, J. Phys.: Condens. Matter **4**, 15 (1991).
 - [19] M. J. P. Nijmeijer and C. Bruin, J. Chem. Phys. **103**, 8201 (1995); C. Bruin, M. J. P. Nijmeijer, and R. M. Crevecoeur, J. Chem. Phys. **102**, 7622 (1995).
 - [20] J. Z. Tang and J. G. Harris, J. Chem. Phys. **103**, 8201 (1995); J. G. Harris, J. Chem. Phys. **105**, 4889 (1996).
 - [21] F. Varnik, J. Baschnagel, and K. Binder, J. Chem. Phys. **113**, 4444 (2000).
 - [22] R. Shuttleworth, Proc. Phys. Soc. A **63**, 444 (1950).
 - [23] B. B. Laird and R. L. Davidchack, J. Chem. Phys. **132**, 204101 (2010).
 - [24] W. A. Tiller, *The Science of Crystallization: Microscopic Interfacial Phenomena* (Cambridge Univ. Press, New York, 1991).
 - [25] D. Deb, A. Winkler, M. H. Yamani, M. Oettel, P. Virnau, and K. Binder, J. Chem. Phys. **134**, 214706 (2011).
 - [26] D. Deb, D. Wilms, A. Winkler, P. Virnau, and K. Binder,

- Int. J. Mod. Phys. C (2012).
- [27] F. Leroy, Daniel J. V. A. dos Santos, and F. Müller-Plathe, *Macromol. Rapid Commun.* **30**, 864 (2009); F. Leroy and F. Müller-Plathe, *J. Chem. Phys.* **133**, 044110 (2010).
- [28] M. Heni and H. Löwen, *Phys. Rev. E* **60**, 7057 (1999).
- [29] A. Fortini and M. Dijkstra, *J. Phys.: Condens. Matter* **2006**, 18, L371.
- [30] B. B. Laird and R. L. Davidchack, *J. Phys. Chem. C* **111**, 15952 (2007).
- [31] R. Benjamin and J. Horbach, *J. Chem. Phys.* **137**, 044707 (2012).
- [32] C. Jarzynski, *Phys. Rev. Lett.* **78**, 2690 (1997).
- [33] C. Jarzynski, *Phys. Rev. E* **73**, 046105 (2006).
- [34] R. F. Fox, *Proc. Natl. Acad. Sci. USA* **100**, 12537 (2003).
- [35] M. R. Shirts and V. S. Pande, *J. Chem. Phys.* **122**, 144107 (2005).
- [36] C. H. Bennett, *J. Comput. Phys.* **22**, 245 (1976).
- [37] Y. Mu and X. Song, *J. Chem. Phys.* **124**, 034712 (2006).
- [38] R. L. Davidchack, *J. Chem. Phys.* **133**, 234701 (2010).
- [39] B. B. Laird, R. L. Davidchack, Y. Yang, and M. Asta, *J. Chem. Phys.* **131**, 114110 (2009).
- [40] J. W. Cahn, in *Interfacial Segregation, Ed.: W C. Johnson and J. M. Blakeley* (American Society for Metals, Metals Park, OH, 1979), pp. 3-23.
- [41] J. W. Gibbs, *The Collected Works* (Yale University Press, New Haven, CT, 1957), Vol. 1.
- [42] T. Young, *Phil. Trans. R. Soc.* **95**, 65 (1805).
- [43] J. Q. Broughton and G. H. Gilmer, *J. Chem. Phys.* **84**, 5759 (1986).
- [44] R. L. Davidchack and B. B. Laird, *J. Chem. Phys.* **118**, 7651 (2003).
- [45] Y. Asano and K. Fuchizaki, *J. Chem. Phys.* **137**, 174502 (2012).
- [46] Y. Asano and K. Fuchizaki, *J. Phys. Soc. Jpn.* **78**, 055002 (2009).
- [47] W. H. Press, B. P. Flannery, S. A. Teukolsky, and W. T. Vetterling, *Numerical Recipes in FORTRAN*, 2nd ed. (Cambridge University Press, Cambridge, U.K., 1992).
- [48] T. Frolov and Y. Mishin, *Phys. Rev. B* **79**, 045430 (2009).
- [49] T. Frolov and Y. Mishin, *J. Chem. Phys.* **131**, 054702 (2009).
- [50] S. Kim, Y. W. Kim, P. Talkner, and J. Yi, *Phys. Rev E* **86**, 041130 (2012).